

On estimation of entrance boundary parameters from downstream measurements using adjoint approach

A. K. Alekseev*¹

RSC 'ENERGIA', Korolev, Moscow Region, 141070, Russian Federation

SUMMARY

An estimation of entrance boundary conditions from the downstream measurements is considered in variational statement form for two-dimensional supersonic laminar flow. The adjoint problem is used for the calculation of the discrepancy gradient in space of control parameters. The numerical tests presented demonstrate the successful estimation of boundary parameters of spatial distribution by using gradient methods. Copyright © 2001 John Wiley & Sons, Ltd.

KEY WORDS: adjoint problem; parabolized Navier–Stokes; parameter estimation

1. INTRODUCTION

The present state of experimental art provides abundant data on spatial distributions of velocity components, temperature density, and concentrations in the flow field [1–3]. These methods provide high spatial resolution and high accuracy. Nevertheless the direct measurement of flow parameters in regions of interest may be difficult, for example, due to lack of access. The measurements may be located in some other zones. On the other hand, the estimation of the total flow field from measurements in some section may be of interest. Both these problems may be reduced to the estimation of entrance boundary parameters from measurements in a downstream flow field section (or set of sections). This problem may be posed in variational statement form, where the discrepancy between measured and calculated flow parameters is minimized. Gradient methods (steepest descent, conjugate gradient, quasi-Newton) are often used for the minimization, the discrepancy (residual) gradient calculation being the most time-consuming element of these methods. When the

* Correspondence to: Yaroslavskoe shosse 178, apt. 94, Puskindo 2, Moscow Region 141200, Russian Federation.

¹ E-mail: aleksey.alekseev@relcom.ru

number of control parameters is small, the calculation of the gradient by direct numerical differences may be used. Under this approach, the number of forward problem solutions (main code runs) is proportional to the number of control parameters. At the large number of control parameters, the adjoint approach is more efficient [4–13]. It requires the solution of only one forward and one adjoint problem (with the computation time close to the forward one) for gradient calculation. Adjoint problems are used for a large set of optimum design, flow control, and parameter estimation problems. The minimum drag body design was studied in Reference [7] using the two-dimensional incompressible laminar Navier–Stokes and in Reference [8] using the Reynolds-averaged compressible Navier–Stokes. The flow control problems are considered in References [9–11] using different statements. The parameter estimation problems (initial or boundary conditions, coefficients) are considered for data assimilation in atmosphere and ocean dynamics for incompressible flows [12]. The determination of entrance temperature from the outflow boundary temperature measurements is considered for supersonic flow in Reference [13].

The estimation of unknown entrance parameters (temperature, density, and velocity components) from measurements within a flow field using adjoint problem and gradient optimization is the main topic of present study.

2. STATEMENT OF PROBLEM

The estimation of unknown parameters ($f_\infty(Y) = (\rho(Y), U(Y), V(Y), T(Y))$) on the entrance boundary (Figure 1) from measurements in a flow field section $f^{\text{exp}}(X_m, Y_m)$ is considered in the variational statement. The discrepancy of measured and calculated flow parameters is minimized. The algorithm under consideration consists of the flow field calculation (forward problem), the discrepancy gradient computation using forward and adjoint problems and the gradient optimization method.

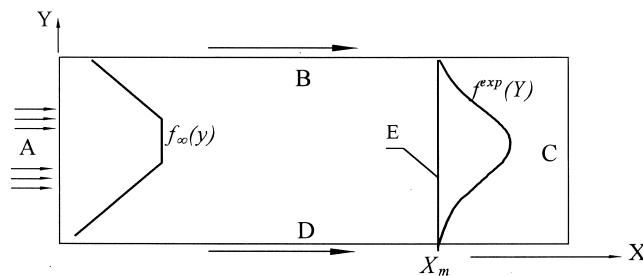


Figure 1. Flow sketch. Entrance boundary E section of measurements.

3. FORWARD PROBLEM

The two-dimensional parabolized Navier–Stokes equations are used herein in the form similar to that in Reference [14]. The flow (Figure 1) is laminar and supersonic along the X co-ordinate

$$\frac{\partial(\rho U)}{\partial X} + \frac{\partial(\rho V)}{\partial Y} = 0 \quad (1)$$

$$U \frac{\partial U}{\partial X} + V \frac{\partial U}{\partial Y} + \frac{1}{\rho} \frac{\partial P}{\partial X} = \frac{1}{Re} \frac{\partial^2 U}{\partial Y^2} \quad (2)$$

$$U \frac{\partial V}{\partial X} + V \frac{\partial V}{\partial Y} + \frac{1}{\rho} \frac{\partial P}{\partial Y} = \frac{4}{3\rho Re} \frac{\partial^2 V}{\partial Y^2} \quad (3)$$

$$U \frac{\partial e}{\partial X} + V \frac{\partial e}{\partial Y} + (\kappa - 1)e \left(\frac{\partial U}{\partial X} + \frac{\partial V}{\partial Y} \right) = \frac{1}{\rho} \left(\frac{\kappa}{Re Pr} \frac{\partial^2 e}{\partial Y^2} + \frac{4}{3 Re} \left(\frac{\partial U}{\partial Y} \right)^2 \right) \quad (4)$$

$$P = \rho RT, \quad e = C_v T = \frac{R}{(\kappa - 1)T}, \quad (X, Y) \in \Omega = (0 < X < X_{\max}; 0 < Y < 1)$$

The entrance boundary conditions (A ($X = 0$); Figure 1) are as follows:

$$e(0, Y) = e_{\infty}(Y), \quad \rho(0, Y) = \rho_{\infty}(Y), \quad U(0, Y) = U_{\infty}(Y), \quad V(0, Y) = V_{\infty}(Y) \quad (5)$$

The outflow condition

$$\frac{\partial f}{\partial Y} = 0$$

is used on B, D ($Y = 0, Y = 1$).

These equations form the ‘forward’ problem, enabling the flow field calculation from the known inflow boundary data.

4. ADJOINT PROBLEM

The flow parameters at some set (sections in present paper) of the flow field points $f^{\text{exp}}(X_m, Y_m)$ are available. The values $f_{\infty}(Y) = (\rho(Y), U(Y), V(Y), e(Y))$ on the boundary A are unknown and must be determined. For this purpose we minimize the discrepancy between computed and measured values $f^{\text{exp}}(X, Y)$ on the set of measurement points

$$\varepsilon(f_{\infty}(Y)) = \int_0^{X_{\max}} \int_0^1 (f^{\text{exp}}(X, Y) - f(X, Y))^2 \delta(X - X_m) \delta(Y - Y_m) dX dY \quad (6)$$

The gradient methods are used herein for the discrepancy minimization. The solution of the adjoint problem is the fastest way for the discrepancy gradient calculation when the number of control parameters is relatively large [5,6,8,9,11,13]. The continuous approach (engendering system of partial differential equations (PDE)) to the adjoint problem statement is used herein. According to References [4–6], we define the Lagrangian $L(f_\infty, f, \Psi)$ using the weak form of the problem (1)–(4) and discrepancy (6)

$$\begin{aligned}
 L(f_\infty, f, \Psi) = & \varepsilon(f_\infty(Y)) + \iint_{\Omega} \left(\frac{\partial(\rho U)}{\partial X} + \frac{\partial(\rho V)}{\partial Y} \right) \Psi_\rho(X, Y) \, dX \, dY \\
 & + \iint_{\Omega} \left(U \frac{\partial U}{\partial X} + V \frac{\partial U}{\partial Y} + \frac{1}{\rho} \frac{\partial P}{\partial X} - \frac{1}{Re \rho} \frac{\partial^2 U}{\partial Y^2} \right) \Psi_U(X, Y) \, dX \, dY \\
 & + \iint_{\Omega} \left(U \frac{\partial V}{\partial X} + V \frac{\partial V}{\partial Y} + \frac{1}{\rho} \frac{\partial P}{\partial Y} - \frac{4}{3 Re \rho} \frac{\partial^2 V}{\partial Y^2} \right) \Psi_V(X, Y) \, dX \, dY \\
 & + \iint_{\Omega} \left(U \frac{\partial e}{\partial X} + V \frac{\partial e}{\partial Y} + (\kappa - 1)e \left(\frac{\partial U}{\partial X} + \frac{\partial V}{\partial Y} \right) - \frac{\kappa}{\rho Re Pr} \frac{\partial^2 e}{\partial Y^2} \right. \\
 & \left. - \frac{4}{3 Re \rho} \left(\frac{\partial U}{\partial Y} \right)^2 \right) \Psi_e(X, Y) \, dX \, dY
 \end{aligned} \tag{7}$$

Herein the adjoint parameters (Lagrange multipliers) $(\Psi_\rho(X, Y), \Psi_U(X, Y), \Psi_V(X, Y), \Psi_e(X, Y)) \in H^{1,2}(\Omega)$; $(H^{1,2}(\Omega))$ is the Hilbert space of functions having derivatives of first- (X) and second-order (Y).

The objective of transformations is to find functions $\Psi_\rho, \Psi_U, \Psi_V, \Psi_e$, such that $\Delta \varepsilon = \Delta L = \int_Y \text{grad}(\varepsilon) \Delta f_\infty(Y) \, dY$, while all other first-order terms equal zero (it may be shown that $\partial L / \partial f_\infty = d\varepsilon / df_\infty$ [11]).

We state the tangent problem in order to determine the dependence of the Lagrangian variation on the change of control parameters. We change the entrance boundary condition (5) by an increment

$$\Delta f(0, Y) = \Delta f_\infty(Y) \tag{8}$$

and determine the corresponding increments of $\Delta \rho, \Delta U, \Delta V, \Delta e$ in Equations (1)–(4) by subtracting undisturbed values. After that, we consider the Lagrangian (7) variation with an account of the incremental equations for $\Delta \rho, \Delta U, \Delta V, \Delta e$ by subtracting undisturbed values and accounting only first-order members. After rearranging terms with $\Delta \rho, \Delta U, \Delta V, \Delta e$, we integrate the result by parts and use boundary conditions for increments. As a result, the following adjoint problem is stated:

$$\begin{aligned}
 & U \frac{\partial \Psi_\rho}{\partial X} + V \frac{\partial \Psi_\rho}{\partial Y} + (\kappa - 1) \frac{\partial(\Psi_V e / \rho)}{\partial Y} + (\kappa - 1) \frac{\partial(\Psi_U e / \rho)}{\partial X} - \frac{\kappa - 1}{\rho} \left(\frac{\partial e}{\partial Y} \Psi_V + \frac{\partial e}{\partial X} \Psi_U \right) \\
 & + \left(\frac{1}{\rho^2} \frac{\partial P}{\partial X} - \frac{1}{\rho^2 Re} \frac{\partial^2 U}{\partial Y^2} \right) \Psi_U + \frac{1}{\rho^2} \left(\frac{\partial P}{\partial Y} - \frac{4}{3 Re} \frac{\partial^2 V}{\partial Y^2} \right) \Psi_V
 \end{aligned}$$

$$-\frac{1}{\rho^2} \left(\frac{\kappa}{Re Pr} \frac{\partial^2 e}{\partial Y^2} + \frac{4}{3 Re} \left(\frac{\partial U^2}{\partial Y} \right)^2 \right) \Psi_e + 2(\rho^{\exp}(X, Y) - \rho(X, Y)) \delta(X - X_m) \delta(Y - Y_m) = 0 \quad (9)$$

$$U \frac{\partial \Psi_U}{\partial X} + \frac{\partial(\Psi_U V)}{\partial Y} + \rho \frac{\partial \Psi_\rho}{\partial X} - \left(\frac{\partial V}{\partial X} \Psi_U + \frac{\partial e}{\partial X} \Psi_e \right) + \frac{\partial}{\partial X} \left(\frac{P}{\rho} \Psi_e \right) + \frac{\partial^2}{\partial Y^2} \left(\frac{1}{\rho Re} \Psi_U \right) - \frac{\partial}{\partial Y} \left(\frac{8}{3 Re} \frac{\partial U}{\partial Y} \Psi_e \right) + 2(U^{\exp}(X, Y) - U(X, Y)) \delta(X - X_m) \delta(Y - Y_m) = 0 \quad (10)$$

$$\frac{\partial(U \Psi_V)}{\partial X} + V \frac{\partial \Psi_V}{\partial Y} - \left(\frac{\partial U}{\partial Y} \Psi_U + \frac{\partial e}{\partial Y} \Psi_e \right) + \rho \frac{\partial \Psi_\rho}{\partial Y} + \frac{\partial}{\partial Y} \left(\frac{P}{\rho} \Psi_e \right) + \frac{4}{3 Re} \frac{\partial^2}{\partial Y^2} \left(\frac{\Psi_V}{\rho} \right) + 2(V^{\exp}(X, Y) - V(X, Y)) \delta(X - X_m) \delta(Y - Y_m) = 0 \quad (11)$$

$$\frac{\partial(U \Psi_e)}{\partial X} + \frac{\partial(V \Psi_e)}{\partial Y} - \frac{\kappa - 1}{\rho} \left(\frac{\partial \rho}{\partial Y} \Psi_U + \frac{\partial \rho}{\partial X} \Psi_U \right) - (\kappa - 1) \left(\frac{\partial U}{\partial X} + \frac{\partial V}{\partial Y} \right) \Psi_e + (\kappa - 1) \frac{\partial \Psi_V}{\partial Y} + (\kappa - 1) \frac{\partial \Psi_U}{\partial X} + \frac{\kappa}{Re Pr} \frac{\partial^2}{\partial Y^2} \left(\frac{\Psi_e}{\rho} \right) + 2(e^{\exp}(X, Y) - e(X, Y)) \delta(X - X_m) \delta(Y - Y_m) = 0 \quad (12)$$

The boundary conditions on C ($X = Y_{\max}$) are

$$\Psi_f|_{X=Y_{\max}} = 0$$

The following condition is used on B, D ($Y = 0, Y = 1$):

$$\frac{\partial \Psi_f}{\partial Y} = 0 \quad (13)$$

If Equations (9)–(13) are satisfied, then

$$\begin{aligned} \Delta \varepsilon(f_\infty(Y)) = \Delta L(f_\infty(Y)) = & \int_Y ((\Psi_e U + (\kappa - 1) \Psi_U) \Delta e_\infty(Y))|_{X=0} dY \\ & + \int_Y ((\Psi_\rho U + (\kappa - 1) \Psi_U e / \rho) \Delta \rho_\infty(Y))|_{X=0} dY \\ & + \int_Y ((\Psi_U U + \rho \Psi_\rho + (\kappa - 1) \Psi_e e) \Delta U_\infty(Y))|_{X=0} dY \\ & + \int_Y ((\Psi_V U \Delta V_\infty(Y))|_{X=0} dY \end{aligned} \quad (14)$$

This expression (it may be considered as the optimality condition when it equals zero) permits us to calculate the discrepancy gradient in the space of control variables (entrance flow parameters).

It should be noted that the structure of the adjoint problem (9)–(13) and gradient (14) provide a mutual compensation of different control variables. For example, the mismatch in temperature readings engenders non-zero gradients for the inflow velocity component $U_\infty(Y)$. This feature may cause an increase in instability.

The gradient may be obtained from Equation (14) for an almost arbitrary set of input data, which may cause additional problems (stability and uniqueness) if this dataset is not sufficient (small number of points). Hence additional analysis is necessary if the data are located on the irregular set of points. This analysis may be performed using a Hessian spectrum obtained from solution of the second-order adjoint problem [17]. In the present paper we consider only datasets located on the flow sections.

5. GRADIENT CALCULATION

Equation (14) provides the discrepancy gradient estimation from the combination of the flow parameters and adjoint variables

$$\begin{aligned}\frac{\partial \varepsilon}{\partial e_\infty}(Y) &= \Psi_e U + (\kappa - 1) \Psi_U \\ \frac{\partial \varepsilon}{\partial \rho_\infty}(Y) &= \Psi_\rho U + (\kappa - 1) \Psi_U e / \rho \\ \frac{\partial \varepsilon}{\partial U_\infty}(Y) &= \Psi_U U + \rho \Psi_\rho + (\kappa - 1) \Psi_e e \\ \frac{\partial \varepsilon}{\partial V_\infty}(Y) &= \Psi_V U\end{aligned}\tag{15}$$

The flow field (forward problem (1)–(4)) is computed by a finite difference method [15] marching along the X . The method is of first order accuracy X and second order on Y (central differences). The pressure gradient for supersonic flow is computed from energy and density. The same algorithm (and the same grid) is used for the adjoint problem solution, but the march is performed in the reverse direction (beginning at the $X = X_{\max}$).

The grid contains 50 nodes along Y and 30–100 along X . The time of the forward problem computation is about 1 min using the Pentium 133-based computer. The flow parameters on the entrance boundary $f_\infty(Y_i) = f_i$ ($i = 1, \dots, N$) are used as the set of control variables. The input data $f^{\text{exp}}(X_m, Y_i)$ ($i = 1, \dots, N$) are obtained at certain sections, $X_m = \text{constant}$ (E in Figure 1) (two sections are used in several calculations) from the preliminary computation. (This dataset is used for simplicity and may be easily changed.) The data error is modeled by normally distributed random values δf with dispersion $\sigma: f^{\text{exp}} + \delta f$. The flow parameters are $M = 4$, $Re = 1000$.

The discrepancy gradient is computed using both the adjoint problem and direct differentiation. The comparison of the gradients calculated by direct differentiation and from the

adjoint problem is presented in Figure 2 for one of flow parameters (temperature). The behavior of the gradient components for other parameters is similar. The oscillations occur near boundaries at direct differentiation (for a jet with uniform flow [13] these oscillations are significantly smaller if disturbances do not intersect the boundaries B, D).

6. OPTIMIZATION ALGORITHM

The spatial distribution of parameters on the entrance boundary (A) is determined by gradient methods (the steepest descent or conjugate gradient, the latter being much faster but slightly less robust in presence of data error)

$$f_i^{n+1} = f_i^n - \beta^n S_p \quad (i = 1, \dots, N) \quad (16)$$

$$S^n = \nabla \varepsilon^n \text{ for the steepest descent}$$

$$S^n = \nabla \varepsilon^n + \gamma_n S^{n-1}, \quad \gamma_n = \frac{\|\nabla \varepsilon^n\|^2}{\|\nabla \varepsilon^{n-1}\|^2}, \quad \gamma_0 = 0 \text{ for conjugate gradient}$$

Some tests were performed using the quasi-Newton method [16], which provided the best convergence rate.

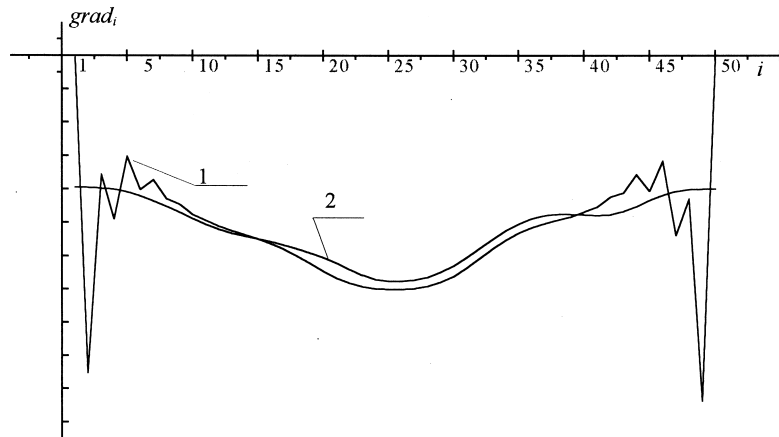


Figure 2. Gradients $\partial \varepsilon / \partial T_\infty(Y_i)$ obtained by direct differentiating and from the adjoint problem for $T_\infty(Y_i)$ (i is the node number): 1, direct differentiating; 2, adjoint problem.

7. NUMERICAL TESTS FOR INFLOW DATA ESTIMATION

The computations have the following structure: the forward problem (1)–(5) is solved for parameter $f(Y_\infty)$ and the flow field $\rho(X, Y)$, $U(X, Y)$, $V(X, Y)$, $T(X, Y)$ is stored. The discrepancy $\varepsilon^n(f)$ is calculated and a stopping criterion is checked. If it is not satisfied the adjoint problem (10)–(14) is solved and the gradient $\text{grad}(\varepsilon^n)$ is calculated from Equation (15). Then the iteration step β^n is determined and the new control parameters are calculated according to Equation (16). The iterations are stopped at $\delta < \sigma_0$, ($\delta = (\varepsilon/N)^{0.5}$ is the normalized discrepancy, σ_0 is the data error) providing the implicit regularization based on the ‘discrepancy’ principle [5,6].

Figure 3 demonstrates the estimation of all flow parameters $f_\infty(Y_i)$ (ρ , U , V , T) ($X/Y = 1.2$, $N_x = 30$, $N_y = 50$) for exact input data ($\sigma = 0$, iterations are stopped at $\delta = 10^{-4}$) and smooth inflow profiles. The values $f_\infty(Y_i)$ (ρ , U , T) are normalized by their minimal value (V is divided by U_{\min} and shifted by unit ($f_v = 1 + V/U_{\min}$)). The solution is smooth for exact data and rippled for data with errors, $\sigma = 0.01$. The data error significantly increases the problem instability. The solution is practically destroyed for $\sigma = 0.05$.

For less smooth inflow profiles, the oscillations occur even for exact input data. Figure 4 demonstrates the estimation of all flow parameters $f_\infty(Y_i)$ (ρ , U , V , T) for exact input data. The instability develops as the discrepancy diminishes. This result may be considered as an illustration of this problem’s ill posedness. At $\delta < 10^{-3}$ the gradient methods stop converging due to large oscillations in flow parameters.

The use of input data from additional sections slightly increases the stability due to measurement error averaging, but the effect is not significant. Hence the Tikhonov regularization

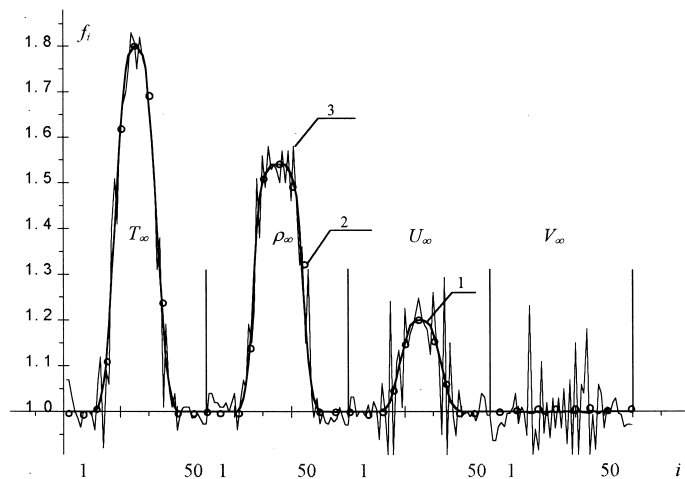


Figure 3. Estimation of underexpanded jet parameters $f_\infty(Y_i)$ from $f^{\text{exp}}(Y_i)$: 1, exact inflow data; 2, $\sigma = 0$; 3, $\sigma = 0.01$.

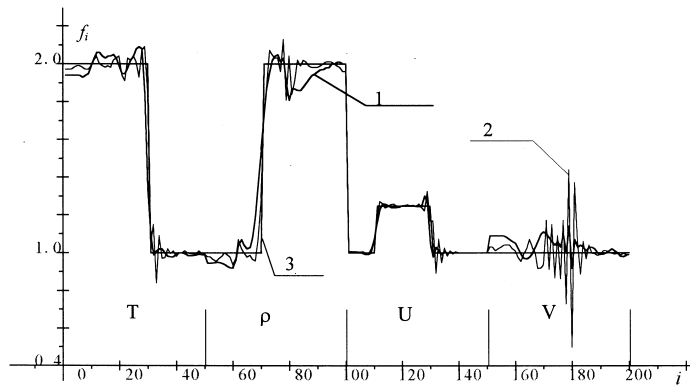


Figure 4. The estimation of entrance boundary parameters $f_{\infty}(Y_i)$ for errorless data at diminishing discrepancy: 1, discrepancy = 0.03; 2, discrepancy = 0.003; 3, exact inflow data.

term of second-order $\alpha(f_{i+1} - 2f_i + f_{i-1})^2$ is added to the discrepancy $\varepsilon(f)$ [18]. The corresponding results are presented in Figure 5 ($\alpha = 0.1$) and demonstrate the more obvious stabilization at $\sigma = 0.05$.

The instability is significantly lower if only a single flow parameter (temperature, for example) is determined while all others are known. Results of $T_{\infty}(Y_i)$ estimation using 'measurements' of $T^{\text{exp}}(Y)$ are presented in Figure 6 for data with errors $\sigma = 0$ and 0.01. The

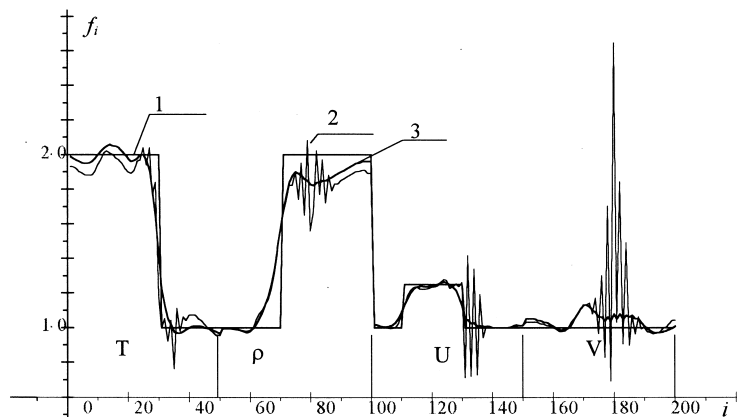


Figure 5. The influence of second-order regularization on the quality of estimation of underexpanded jet parameters $f_{\infty}(Y_i)$ from $f^{\text{exp}}(Y_i)$: 1, exact; 2, $\sigma = 0.01$, without regularization; 3, $\sigma = 0.01$, with regularization.

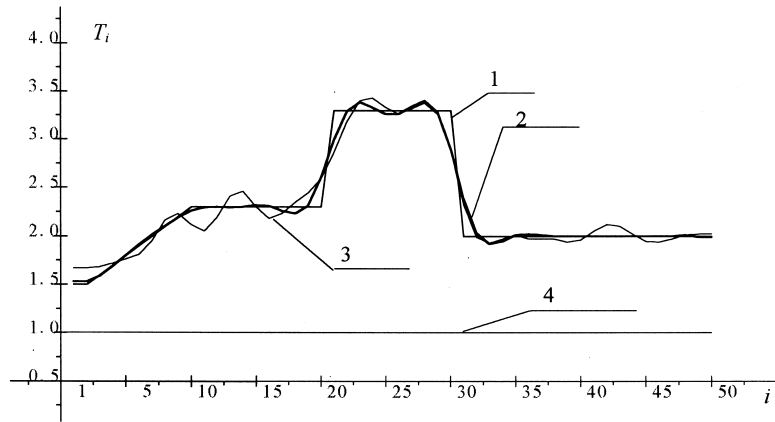


Figure 6. The estimation of $T_{\infty}(Y_i)$ from $T^{\text{exp}}(Y_i)$: 1, exact inflow data; 2, $\sigma = 0.0$; 3, $\sigma = 0.01$; 4, initial guess.

spatially constant temperature is used as the initial guess. At exact input data, the discrepancy diminishes below $\delta = 0.0001$ without significant oscillations. At noisy data, the gradient methods stop at the discrepancy close to the data error. Figure 7 represents results of regularization for data error $\sigma = 0.05$.

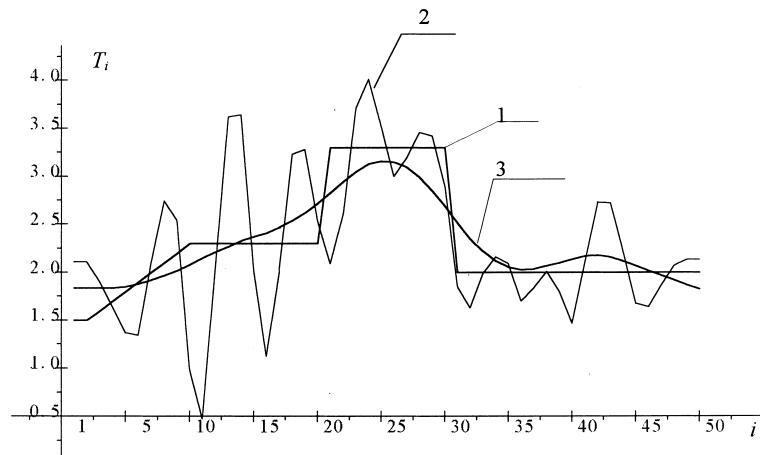


Figure 7. Estimation of $T_{\infty}(Y_i)$ from $T^{\text{exp}}(Y_i)$ with regularization: 1, exact inflow data; 2, $\sigma = 0.05$; 3, $\sigma = 0.05 + \text{regularization}$.

8. CONCLUSION

The estimation of inflow parameters from downstream measurements may be successfully performed using gradient methods of optimization. The solution of the adjoint problem provides the precise calculation of the discrepancy gradient, taking about twice as long as the forward problem solution. The numerical tests demonstrate the successful estimation of inflow parameters for both noiseless and noisy data.

The instabilities caused by this problem's ill posedness may be successfully handled using the 'discrepancy' principle (stopping at discrepancy magnitude close to data error) for moderate data errors. At large data errors, the additional Tikhonov regularizing terms of second-order are efficient.

APPENDIX A. NOMENCLATURE

e	specific energy, $C_v T$
f	flow parameters (ρ, U, V, e)
i	node number along transversal co-ordinate
L	reference length
M	Mach number ($M = U_\infty / (\kappa R T_\infty)^{0.5}$)
P	pressure
Pr	Prandtl number ($Pr = \mu C_v / \lambda$)
R	gas constant
Re	Reynolds number ($Re = \rho_\infty U_\infty L / \mu$)
X, Y	co-ordinates
<i>Greek letters</i>	
α	regularization coefficient
δ	normalized discrepancy
ε	discrepancy of measured and calculated data
κ	specific heat ratio
λ	thermal conductivity
μ	viscosity
σ	input data error
$\Psi_\rho, \Psi_U, \Psi_V, \Psi_e$	adjoint variables
<i>Subscripts</i>	
∞	entrance boundary parameters (control variables)
m	points of measurement
<i>Superscripts</i>	
exp	experimental (target) data

REFERENCES

1. Thomas AM, Barker PF, McIntyre TJ, Rubinsztein-Dunlop H. Velocimetry and thermometry of supersonic flow around a cylindrical body. *AIAA Journal* 1998; **36**(6): 1055–1060.
2. Jiang LY, Sisljan JP. Velocity and density measurements in supersonic high temperature exhaust plumes. *AIAA Journal* 1998; **36**(7): 1216–1222.
3. Clancy PS, Samimi Mo. Two component planar Doppler velocimetry in high speed flows. *AIAA Journal* 1997; **35**(11): 1729–1738.
4. Lions JL. *Optimal Control of Systems Governed by Partial Differential Equations*. Springer: Berlin, 1971.
5. Vasiliev FP. *Methods for Extreme Problems Solution*. Nauka: Moscow, 1981 (in Russian).
6. Alifanov OM, Artyukhin EA, Rummyantsev SV. *Extreme Methods for Solving Ill-posed Problems with Applications to Inverse Heat Transfer Problems*. Begell House Inc.: New York, 1996.
7. Pironneau O. On optimum design in fluid mechanics. *Journal of Fluid Mechanics* 1974; **64**(1): 97–110.
8. Somarwoto B. The variational method for aerodynamic optimization using the Navier–Stokes equations. ICASE Report No. 97-71, 1997.
9. Sahrapour A, Ahmed NU, Tavoularis S. Boundary control of the Navier–Stokes equations with potential application to artificial hearts. In *Second Annual Conference of the CFD Society of Canada*, Toronto, Ontario, Gottlieb JJ, Ethier CR (eds), 1994; 387–394.
10. Joslin RD, Gunzburger MD, Nicolaides RA, Erlebacher G, Hussaini MY. Self-contained, automated methodology for optimal flow control. *AIAA Journal* 1997; **35**(5): 816–824.
11. Clerc M, Le Tallec P, Mallet M. Controle optimal de Navier–Stokes parabolize. INRIA Report No. 2653, 1995.
12. Le Dimet FX, Talagrand O. Variational algorithms for analysis and assimilation of meteorological observations. *Tellus* 1986; **38**(2): 97–110.
13. Alekseev AK. On discrepancy gradient calculation at inflow temperature estimation from outflow data. In *Dynamical Systems Identification and Inverse Problems—III*. Moscow–St. Petersburg, May–June, Alifanov OM (ed.), 1998; 433–443.
14. Anderson DA, Tannehill JC, Pletcher RH. *Computational Fluid Mechanics and Heat Transfer*, vol. 2. Hemisphere: New York, 1988.
15. Alekseev AK. Freestream parameters estimation using heat flux measurements. *AIAA Journal* 1997; **35**(7): 1238–1240.
16. Liu DC, Nocedal J. On the limited memory BFGS method for large scale minimization. *Mathematical Programming* 1989; **45**: 503–528.
17. Vang Z, Navon IM, Le Dimet FX, Zou X. The second order adjoint analysis: theory and applications. *Meteorological and Atmospheric Physics* 1992; **50**: 3–20.
18. Tikhonov AN, Arsenin VYa. *Solution of Ill-posed Problems*. Halsted Press: New York, 1979.